Integrating sphere effective optical path length calibration by gas absorption spectroscopy

**Qiang Gao · Yungang Zhang · Jia Yu ·
Zhiguo Zhang · Shaohua Wu · Wei Guo**

Abstract A method of integrating sphere effective optical path length (EOPL) evaluation using tunable diode laser absorption spectroscopy for gas detection was demonstrated. Oxygen was used as a sample gas for an 8.38 cm diameter integrating sphere calibration; 393.7 ± 1.3 cm EOPL was obtained from the wavelength modulation spectroscopy with second harmonic calibration by measuring oxygen P11 line at 764 nm, which is in agreement with that of 393 cm by using direct absorption spectroscopy calibration. The EOPL calibration accuracy of this method can reach 0.33 %. It has been justified that the EOPL of an integrating sphere is independent of the incident light intensity.

1 Introduction

Gas absorption spectroscopy including differential optical absorption spectroscopy (DOAS), differential absorption lidar (DIAL), Fourier transform infrared spectroscopy (FTIR) and tunable diode laser absorption spectroscopy (TDLAS), etc., has been widely used in monitoring a

Q. Gao (✉) · Y. Zhang · J. Yu · Z. Zhang
Condensed-Matter Science and Technology Institute, Harbin Institute of Technology, Harbin 150001, China
e-mail: gaoqiang429@126.com

Z. Zhang
e-mail: zhangzhiguo@hit.edu.cn

Q. Gao · Y. Zhang · J. Yu · Z. Zhang · S. Wu
Institute of Combustion Engineering, Harbin Institute of Technology, Harbin 150001, China

W. Guo
Chinatech Talroad Technology Co., Ltd., Beijing 100085, China

variety of gases in the fields of environmental monitoring, biomedical applications and industrial process control [1–4]. One of the most important parameters among all the absorption spectroscopic techniques is sensitivity. In order to increase the sensitivity, the light source with low fluctuation and detectors with low dark noise can be employed. Meanwhile, wavelength modulation technology could greatly improve the sensitivity by increasing the signal-to-noise ratio. But according to Beer–Lambert law, one direct and efficient method to improve the sensitivity is to increase the optical path length. A number of techniques have been used to increase the optical path length. One category involves multi-pass cells designed by White, Herriott and Chernin [5–7], which allow a collimated beam of light reflects a number of times between two or more mirrors to increase the gas absorption path length. The second category is cavity enhance techniques including integrated cavity output spectroscopy (ICOS) where the absorption signal is obtained through the integration of the total signal transmitted through optical cavity absorption cell [8], the cavity ring down spectroscopy (CRDS) where gas concentration is calculated by measuring the decay time of pulses in the cavity [9]. Each technique has its own distinctive advantages. However, both multi-pass cells and the cavity enhance techniques share several common problems. The critical alignment of the optical components often induces sophisticated designs of the system which will increase the difficulties to maintain the system tolerance in complex application condition. The interference fringes resulting from Fabry–Pérot etalons between reflecting mirrors are time consuming to reduce [10]. Thus, attention has grown in the utilization of integrating sphere as gas absorption cell.

The integrating sphere can be used as a multi-pass absorption cell where the input light transports through

several reflections before exiting the sphere. This results in an optical path length enhancement which is several times longer than the diameter of the integrating sphere. High-quality commercial integrating spheres have high-reflection internal coating and standard spherical cavity geometry. Ideal Lambertian diffuse scatter such as Spectralon^{TM} ensures a constant irradiance E (W m^{-2}) over the entire spherical geometry cavity which brings low requirements for the laser collimation and alignment and also avoids the emergence of interfere fringes. At present, the use of integrating spheres for gas detection has long been of interest, which has been used for detecting gases such as monoxide, carbon dioxide, ammonia, water vapor and methane. [11, 12]. For all the applications of integrating sphere in gas sensing, the EOPL is a significant parameter to calculate the concentration of the target gas. Thus, accurate evaluation of EOPL is of great importance.

Using integrating sphere as a gas absorption cell, the EOPL of an integrating sphere, not like the traditional optical cell which can be obtained by measuring the length directly, highly depends on the precise manufacturing and setup of the sphere, being highly sensitive to small changes in the internal reflectivity and port fraction. Previous works concerning the evaluation of EOPL include theoretical calculation based on light propagation theory in the integrating spheres [13] and the measurement of the decay time of a pulse laser [14]. In 2009, Hodgkinson et al. [15] gave out the EOPL based on Beer–Lambert law by measuring the normalized transmission of a certain concentration of methane using direct absorption spectroscopy.

In this paper, an EOPL calibration curve of the integrating sphere was demonstrated using gas absorption spectroscopy. Comparison of two EOPL results was illustrated between direct absorption detection and second harmonic absorption detection. The EOPL of the integrating sphere could be obtained from the measurement even with no detailed knowledge of the integrating sphere or the absorption cross section of the sample gas. The calibration accuracy of EOPL was discussed.

2 Theory

In the ideal case, for a good quality commercial integrating sphere with standard spherical cavity geometry, the radiance from a given point is a constant in any direction, and after single pass, the irradiance at the sphere walls is perfectly uniform over the surface. The average pass length for a single pass through a close approximate integrating sphere is equal to two-thirds of the diameter [13, 16]. So the effective optical path length can be expressed as

$$L_{\text{eff}} = \frac{2}{3}MD. \tag{1}$$

D is the diameter of the integrating sphere, and M is the multiplier which strongly depends on the reflectivity ρ and port fraction f (sum of all ports areas/surface area of sphere), which can be expressed as follows

$$M = \frac{\rho}{1 - \rho(1 - f)}. \tag{2}$$

Several factors will lead to the inaccuracy of EOPL in using this method. The reflectivity ρ and port fraction f are difficult to be measured precisely. If the reflectivity tends to 100 % and port fraction tends to be infinitely small, a little error in the value of reflectivity and port fraction will lead to large change on EPOL. Some integrating spheres adding baffles in the inner surface break the standard spherical cavity geometry which will lead to invalid theoretical equation of (1) and (2). Thus, the theoretical EOPL will deviate from the true value. Furthermore, gas absorption will also affect the theoretical EOPL, especially when the gases having strong absorption. Although Edward S. Fry et al. have given out a formula considering gas absorption [17], yet the actual EOPL still could not be calibrated out accurately in theoretical method.

The other way is to measure the time constant of the integrating sphere. For typical integrating spheres, time constant is ranging from several nanoseconds to a decade nanoseconds, which usually has 5–10 % errors in the result of time resolution spectroscopy [18]. It will affect the EOPL by the propagation of error. The sophisticated system of measuring time constant also limits its application. For gas detection, the inaccuracy of the EOPL will affect the measured concentration according to Beer–Lambert law. In order to solve the problems and obtain the accurate EOPL of the integrating sphere for gas detecting, an experimental method for EOPL calibrating was presented.

3 Experimental demonstration

In the experiments, A 3.3 inch (8.38 cm) diameter commercial integrating sphere (Labsphere, 3P-GPS-033-SL) with two ports (input and output optical radiation) was modified for use as gas absorption cell. The port fraction is about 0.002. Light ranging from 200 to 1,800 nm wavelength entering the integrating sphere can be scattered by the inner surface with high diffuse reflectance over 95 %. The characteristic absorption lines of a variety of gases within the wavelength range could be used for the EOPL calibration. In this paper, atmospheric oxygen having close-lying and well-resolved absorption lines P11 in the

A-band around 760 nm at room temperature was measured for EOPL calibration.

The experimental configuration of WMS-2f signal measurement of oxygen in the integrating sphere is schematically shown in Fig. 1. A VCSEL diode laser (Laser Components, single-mode VCSEL 763 nm TO46) with a nominal wavelength of 764 nm at 22.58 °C and a free running output power of 0.3 mW was used as the source. The laser injection current was superimposed a 12 kHz sinusoidal ac component which was ramped at repetition of 10 Hz. The modulated laser beam irradiated into the integrating sphere from the input port. A 0.6 mm core optical fiber was embedded in the internal cavity for light collection and then transmitted into a PMT (Hamamatsu, PMTH-S1-1P28). The electronic signal was demodulated by a lock-in-amplifier (SR830) with 1-ms time constant at second harmonic of the modulation frequency (2f, 24 kHz). The data were displayed and recorded by an oscilloscope (Tektronix, DPO5054). In the experiment measuring direct absorption signal of oxygen, the emitted wavelength was scanned across the gas absorption line center using a current ramped by the driver at repetition of 10 Hz. The signal received by PMT was directly recorded and displayed by the oscillograph. Before the experiments of integrating sphere, the direct and second harmonic signals of oxygen with different optical lengths in the open air were measured for calibration. Here, a photodiode detector (Thorlabs, DET10A) was used.

4 Results and discussion

Figure 2 shows the absorption signals of oxygen in the air through a 115 cm optical path length and the integrating sphere, respectively. Figure 2a is the direct absorption signals during a ramp scan without sine modulation. The incident light beam being scattered by the inner surface of
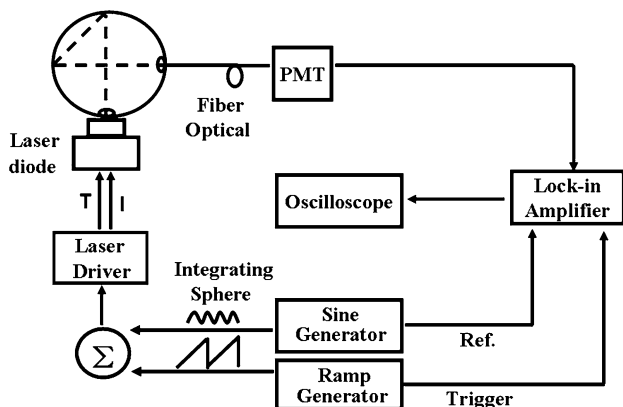

Fig. 1 Schematic diagram of the TDLAS-IS configuration

the integrating sphere will make subsequent random multiple passes across the cell. Thus, the recorded direct absorption signal from the integrating sphere is the superposition of signals under different reflect numbers which is completely different compared with light transportation in the open air. This may cause a broadening of the direct absorption line shape. However, the comparison of the normalized absorption signals and residual plot shown in Fig. 2c indicates that the absorption line shape from the integrating sphere coincides well with that in the open air. In other words, the influence of line shape broadening in the integrating sphere is small enough to be ignored which guarantees our research accuracy on optical path length extension of integrating sphere using wavelength modulation spectroscopy. Figure 2b shows a raw data sample of the recorded demodulated WMS-2f signals during a ramp scan. The WMS-2f signal was defined by dividing the raw WMS-2f signal with the total intensity of the incident laser in order to eliminate incident light amplitude variation. The WMS-2f signal is proportional to the direct absorption signal which varies directly with the concentration of the analyte and the optical path length. In the experiment, a constant concentration of 20.9 % oxygen was measured, so the WMS-2f signal can be considered to represent the optical path length directly.

The EOPL of the integrating sphere was obtained by linear fitting the absorption signals of a series known optical path lengths in the open air with the same concentration of oxygen. WMS-2f signals were measured under several different optical path lengths in the open air ranging from 80 to 200 cm with 20-cm interval. The peak value of the WMS-2f signals versus optical path length is plotted in Fig. 3a. High linearity ($R^2 = 0.9999$) with a slope of 0.280 ± 0.001 and intercept of 0.945 ± 0.242 was obtained from the linear fitting. Because the gas absorption cross section is relatively small, according Beer–Lambert law, the linearity will be available when using integrating sphere as absorption cell ($\alpha L \ll 1$, α is absorption cross section, L is optical pathlength). So the integrating sphere EOPL can be obtained directly from the linear fitting by measuring the WMS-2f signal. The EOPL of the integrating sphere calculated from the linear fitting optical parameters of calibration curve in Fig. 3a was 396.2 ± 0.6 cm. Considering the additional pathlength outside the integrating sphere (including the distance from the integrating sphere to the laser and the detector), 2 cm was subtracted. So the actual EOPL of the integrating sphere was 394.2 ± 0.6 cm. The uncertainty of ±0.6 was caused by the error of both the slope and the intercept. The accuracy of the detecting system will be discussed in detail later. This result indicates the extended EOPL about 47 times longer than the integrating sphere diameter. The result of integrating sphere EOPL calibration using direct

Fig. 2 a Direct absorption signals of oxygen during a ramp scan recorded through the air with 115 cm optical path length, **b** WMS-2f signals of oxygen during a ramp scan recorded through the air with the 8.38 cm diameter integrating sphere. **c** Two normalized absorption signals and residual plot
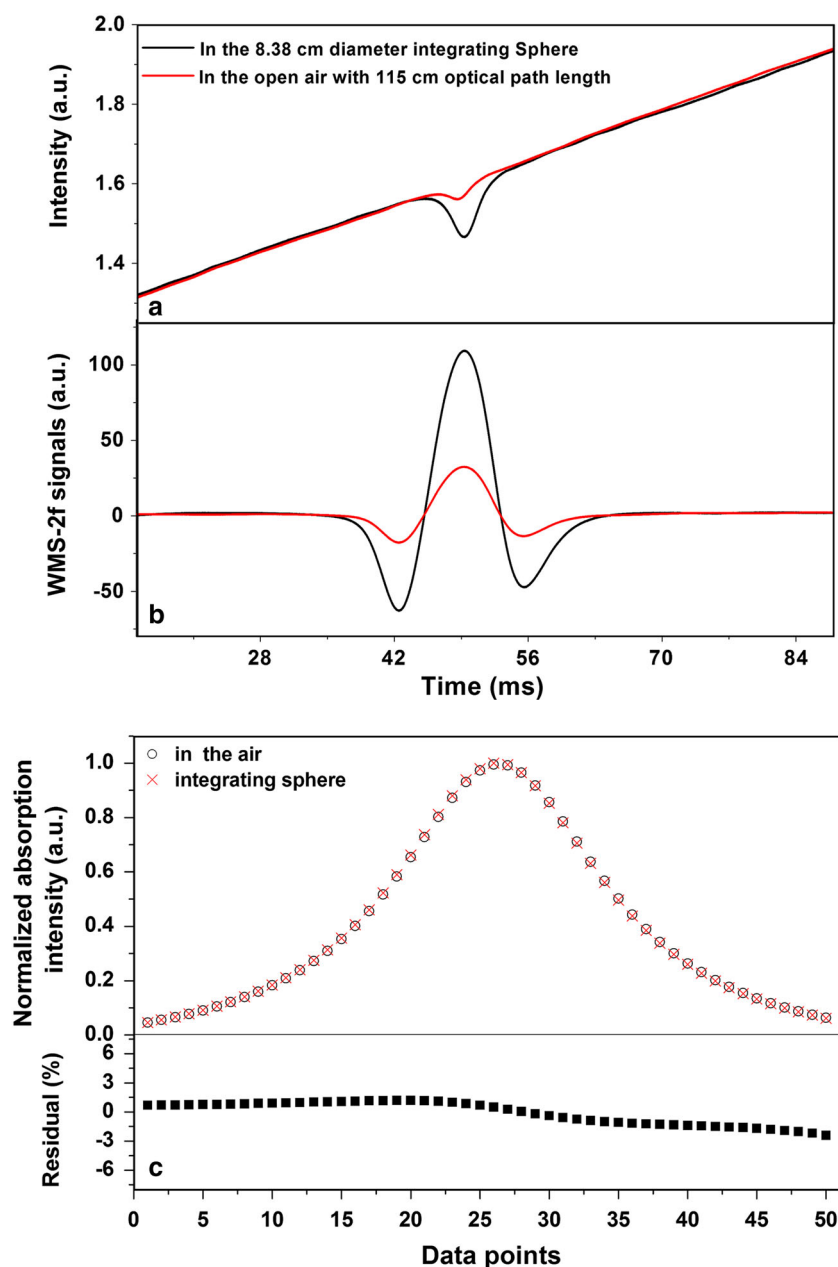

absorption spectroscopy is shown in Fig. 3b. An EOPL of 393 cm was obtained, which is in agreement with that using wavelength modulation spectroscopy. The theoretical EOPL could be obtained according to Eq. 1. The reflectivity is about 98.9 % at the wavelength of 760 nm according to the manufacturer provides and the port fraction 0.002 according to the manual of the integrating sphere. Bring the above factors into Eq. 1, and then, the calculated EOPL is 424 cm.

Figure 4a shows 20 calibrated EOPL points from the integrating sphere by measuring the oxygen in the atmosphere, each measurement taking $\sim$60 s, the EOPL of the integrating sphere in the measurement was 393.7 $\pm$ 1.2 cm. The total systematic error is from two parts. One is the measurement error of $\pm$1.2 cm, and the other is the calibration error of $\pm$0.6 cm calculated from the uncertainty of the slope and the intercept discussed before. So the total error from square average is $\pm$1.3 cm. Thus, the final EOPL of the integrating sphere was 393.7 $\pm$ 1.3 cm, and an accuracy of 0.33 % was obtained. Figure 4b shows the EOPLs with the output voltage (2 MΩ output impedance) by using random incident intensity of the laser and random detection voltage of PMT. The indicant intensity of the laser was changed by a neutral density filter. The error of the EOPL was within expected. It indicates that the intensity of the light source and the
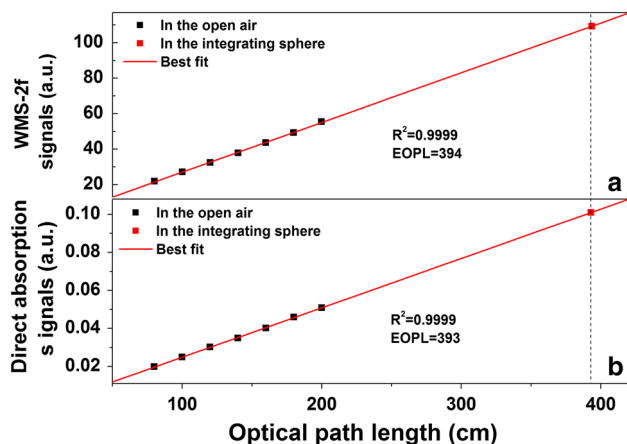
Fig. 3 Calibration plot of optical path length corresponding to oxygen WMS-2f absorption signal (**a**), and direct absorption signal (**b**) obtained in the open air
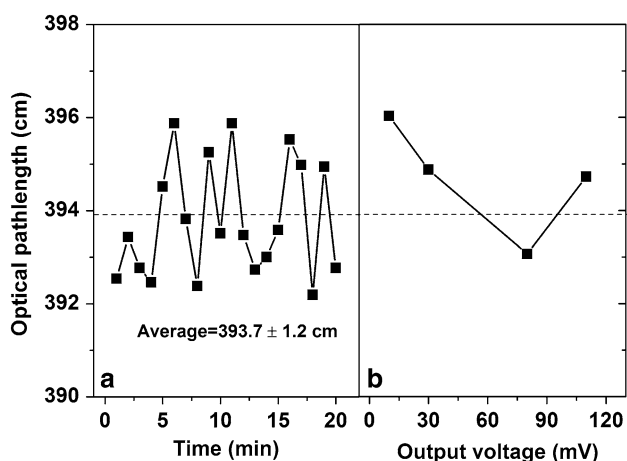
Fig. 4 a The EOPL fluctuation with time; **b** the EOPL with the output voltage using random incident intensity and random detection voltage of PMT

detection voltage of PMT do not affect the calibration result.

From the direct absorption experiments presented in this paper, we can see that no obvious line shape broadening was observed. It can be explained that the time interval of light received by the detector from n times' reflection to $(n + 1)$ times' reflection cannot be recognized. This indicates that at the moment when laser beam was irradiated into the integrating sphere, a unique and constant light field was immediately formed over the sphere's internal surface. As shown in the inset of Fig. 2a, the normalized absorption signal obtained by the integrating sphere and in the open air displayed the same line shape. So if we set the detector and the laser source at a certain distance in the air, the value of direct absorption signal of oxygen will be the same as using integrating sphere. Here, this distance is defined as

equivalent optical path length of the sphere. As a result, the conformity of line shape justifies our method to use the calibration curve of optical path length versus absorption signal in the air to calculate EOPL of the integrating sphere shown in Fig. 3.

As indicated in the results, the experimental EOPL was about 30 cm smaller than the theoretical result. This is mainly due to inaccurate data of the reflectivity and port fraction. So when employing integrating sphere as absorption cell for gas concentration detection, accurate experimental calibration of EOPL is of great importance. J. Hodgkinson et al. [15] give out a revised equation to model gas absorption influence, used direct absorption measurement to get the transmittance of a known concentration of methane and specific absorptivity of the gas ε from HITRAN database, and then calculated the EOPL using Beer–Lambert law. Here in this paper, EOPL was calculated by the calibration curve of absorption signal in the air without knowing the specific absorptivity of gas. Using gas absorption spectroscopy for EOPL calibration, especially using wavelength modulation spectroscopy with second harmonic signal detection, the accuracy will be increased effectively. In addition, the integrating sphere has the ability of anti-light intensity variation and insensitive to alignment issues, which increases the reliability for EOPL calibration. Furthermore, the incident light intensity and the voltage of the PMT do not affect the EOPL, which increase the repeatability of this method. At the same time, this experimental calibration method can measure EOPL of an integrating cavity with arbitrary geometry. Theoretical EOPL expressed by Eq. (1) is only accurate to ideal spherical cavity, so that it needs to be revised in order to get a more accurate value of EOPL when small geometrical shape changes occur such as baffles. Several reports [14, 17] gave out a revised equation to model gas absorption influence of EOPL. We will also discuss the nonlinearity of the Beer–Lambert law to the integrating sphere and the affects of reflectivity and port fraction in detail in future work.

5 Conclusion

In summary, we have established the integrating sphere EOPL calibration method by employing gas absorption spectroscopy, which was demonstrated on oxygen using TDLAS-IS gas detection system. The feasibility of the experimental method by using WMS-2f technology was justified; 393.7 ± 1.3 cm EOPL was obtained, and calibration accuracy of 0.33 % was achieved. Gas absorption spectroscopy for EOPL calibration has the advantages as follows. First, detail knowledge of the integrating sphere is not required, including the reflectance of the inner surface,

port fraction and the diameter of the integrating sphere. Second, this method could be applied to any irregular cavity geometry EOPL calibration. At the same time, this method also provides a reliable alternative for other wavelength EOPL calibration by using the gases having corresponding absorption, especially for those gases having narrow line spectra. However, for those gases having broadband absorption spectra, it is still available to calibrate the EOPL with this method by using direct absorption spectroscopy.

References

1. J. Alnis, U. Gustafsson, G. Somesfalean, S. Svanberg, Appl. Phys. Lett. **76**, 1234–1236 (2000)
2. G. Wysocki, Y. Bakhirkin, S. So, F.K. Tittel, R.Q. Yang, M.P. Fraser, Appl. Opt. **46**, 8202–8210 (2007)
3. S. Svanberg, Appl. Phys. B **92**, 351–382 (2008)
4. X. Liu, J.B. Jeffries, R.K. Hanson, K.M. Hinckley, M.A. Woodmansee, Appl. Phys. B **82**, 469–478 (2006)
5. J.U. White, J. Opt. Soc. Am. **32**, 285–288 (1942)
6. D.R. Herriott, D. Kogelink, H. Kompfner, Appl. Opt. **3**, 523–526 (1964)
7. S.M. Chernin, E.G. Barskaya, Appl. Opt. **30**, 51–58 (1991)
8. A.O. Keefe, J.J. Seherer, J.B. Paul, Chem. Phys. Lett. **307**, 343–349 (1999)
9. J.J. Scherer, J.B. Paul, A. O' Keefe, R.J. Saykally, Chem. Rev. **97**, 25–51 (1997)
10. D. Masiyano, J. Hodgkinson, R.P. Tatam, Appl. Phys. B **90**, 279–288 (2008)
11. E. Hawe, P. Chambers, C. Fitzpatrick, E. Lewis, Meas. Sci. Tehnol. **18**, 3187–3194 (2007)
12. E. Hawe, C. Fitzpatrick, P. Chambers, E. Lewis, J. Opt. A: Pure Appl. Opt. **9**, S12–S18 (2007)
13. J.T.O. Kirk, Appl. Opt. **34**, 4397–4408 (1995)
14. E.S. Fry, J. Musser, G.W. Kattawar, P.W. Zhai, Appl. Opt. **45**, 9053–9065 (2006)
15. J. Hodgkinson*, D. Masiyano and R. P. Tatam, Appl. Opt. **48**, 5748–5758 (2009)
16. S. Tranchart, I.H. Bachir, J.L. Destombes, Appl. Opt. **35**, 7070–7074 (1996)
17. E.S. Fry, G.W. Kattawar, B.D. Strycker, P.W. Zhai, Appl. Opt. **49**, 575–577 (2010)
18. Z.G. Zhang, S. Svanberg, P. Quinet, P. Palmeri, E. Biémont, Phys. Rev. Lett. **87**, 273001 (2001)